

**UCLA**

**UCLA Previously Published Works**

**Title**

Mystery of Three Borides: Differential Metal–Boron Bonding Governing Superhard Structures

**Permalink**

<https://escholarship.org/uc/item/61k3g610>

**Journal**

Chemistry of Materials, 29(23)

**ISSN**

0897-4756

**Authors**

Robinson, Paul J  
Liu, Gaoxiang  
Ciborowski, Sandra  
[et al.](#)

**Publication Date**

2017-12-12

**DOI**

10.1021/acs.chemmater.7b04378

Peer reviewed

# Mystery of Three Borides: Differential Metal-Boron Bonding Governing Superhard Structures

Paul J. Robinson,<sup>†</sup> Gaoxiang Liu,<sup>‡</sup> Sandra Ciborowski,<sup>‡</sup> Chalynette Martinez-Martinez,<sup>‡</sup> Juan R. Chamorro,<sup>‡</sup> Xinxing Zhang,<sup>‡</sup> Tyrel M. McQueen,<sup>‡</sup> Kit H. Bowen,<sup>\*,‡</sup> Anastassia N. Alexandrova<sup>\*,†,§</sup>

<sup>†</sup> Department of Chemistry & Biochemistry, University of California, Los Angeles, Los Angeles, California 90095, United States

<sup>‡</sup> Department of Chemistry and Materials Science, Johns Hopkins University, 3400 N. Charles Street, Baltimore, Maryland 21218, United States

<sup>§</sup> California NanoSystems Institute, Los Angeles, California 90095, United States

**ABSTRACT.** Some transition metal borides are ultra hard. While not harder than diamond, they are easier to process and can be cheaper, sparking intense interest. However, we so far cannot predict which particular borides should be ultra hard. A striking example is the three structurally similar diborides of Ti, Re, and Os, among which only ReB<sub>2</sub> is ultra hard. For this trio, using a combination of theory and experiment done on both the solids and small cluster models, we show that the nature of the metal-boron bonds is the key to hardness, in contrast to the existing theory, which overlooks metal-boron interactions. Ti-B bonding is purely ionic in TiB<sub>2</sub>, and the material yields to shear stress like graphite. OsB<sub>2</sub> is highly covalent, with both bonding and anti-bonding Os-B backbonds present, which weaken the B-network, and ease the OsB<sub>2</sub> yield to compression. ReB<sub>2</sub> has only the bonding Re-B  $\sigma$ -backbond, which strengthens the material against both shear and compression. A general strategy for ultra hard boride design is proposed.

Ultra hard materials have been of interest to human kind since prehistoric times. Borides of certain transition metals form a new class of hard materials.<sup>1-4</sup> Being metals, these borides easily cut with electric discharge machining and thus appear as an attractive alternative to diamond. The governing principles for the design of ultra hard borides have been proposed to be the combination of high electron density at the Fermi level ( $E_F$ ) coming from the metal, making borides incompressible, and a rigid covalent boron skeleton resisting the shear stress.<sup>5-10</sup> The metal and boron sub-lattices in this model are seen independently. Here, we challenge these old principles and show that only with the inclusion of spe-

cific metal-boron bonding can we explain and design for the structure and hardness of borides.

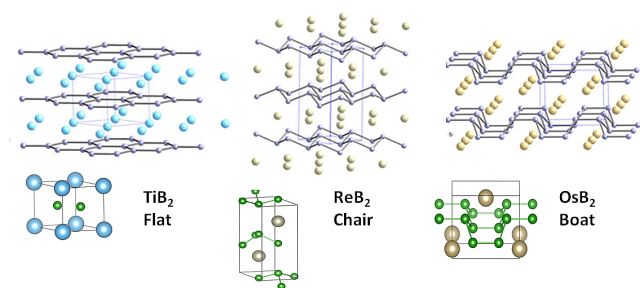


**Figure 1.** The structures of the three borides: TiB<sub>2</sub> featuring a flat B-sheet, and ReB<sub>2</sub> and OsB<sub>2</sub> where the B-sheet is bent in a chair and boat conformations, respectively.<sup>1</sup> The upper images display supercells to make apparent the structural analogies while the lower images show a single unit cell.

We zoom into a set of three diborides, which are stoichiometrically identical, and structurally related yet distinct: TiB<sub>2</sub>, ReB<sub>2</sub>, and OsB<sub>2</sub> (Figure 1). Among these three, only ReB<sub>2</sub> is ultra-hard.<sup>11-15</sup> In all three cases, the boron sub-lattice is a sheet: planar in TiB<sub>2</sub>, and corrugates as a “chair” in ReB<sub>2</sub> and as a “boat” in OsB<sub>2</sub>, by analogy with the conformations of cyclohexane. These diborides demonstrate how boron, a metalloid, is capable of many different kinds of bonds to metals, and this promiscuity strongly dictates hardness.

Our approach links the chemical bonding in materials to that in relevant small cluster fragments, which can be studied in great detail using state-of-the-art theory and experiment. The identified critical elements in the elec-

tronic structure of the cluster are mapped back onto the solid for property rationalization and design.<sup>14,15</sup>

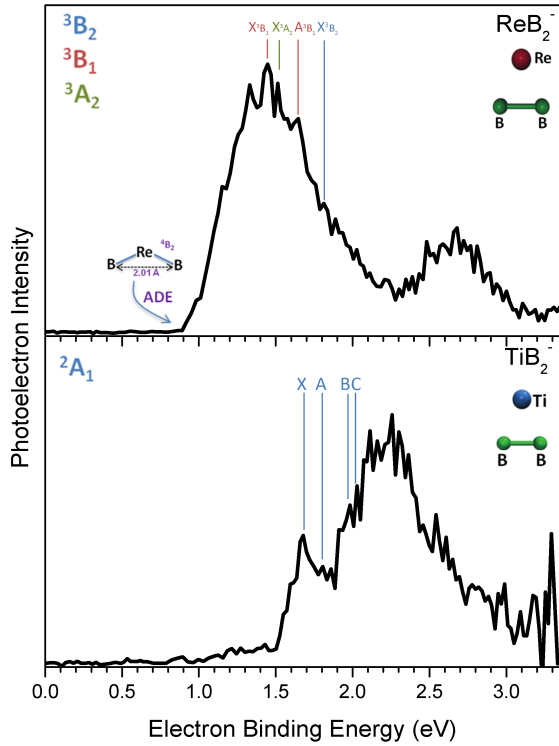


**Figure 2.** The experimental photoelectron spectra of  $\text{ReB}_2^-$  (top) and  $\text{TiB}_2^-$  (bottom), and the theoretical assignment of spectral features.

**Table 1.** The experimental and calculated photoelectron spectra of  $\text{TiB}_2^-$ , and  $\text{ReB}_2^-$  (in eV).

Feature	Expt. E	Transition	Calc. E
<b><math>\text{ReB}_2^-</math></b>			
ADE	$0.9 \pm 0.1$	$^3\text{A}_2 \rightarrow ^4\text{B}_1$	1.21
$\text{X}^1\text{B}_3$	$1.45 \pm 0.1$	$^3\text{B}_1 \rightarrow ^4\text{B}_1$ ( $^3\text{B}_1$ VDE)	1.51
$\text{X}^3\text{A}_2$	$1.52 \pm 0.1$	$^3\text{A}_2 \rightarrow ^4\text{B}_1$ ( $^3\text{A}_2$ VDE)	1.58
$\text{A}^3\text{B}_1$	$1.65 \pm 0.1$	$^3\text{B}_1 \rightarrow ^2\text{B}_1$	1.70
$\text{X}^3\text{B}_2$	$1.76 \pm 0.1$	$^3\text{B}_2 \rightarrow ^4\text{B}_1$ ( $^3\text{B}_2$ VDE)	1.76
<b><math>\text{TiB}_2^-</math></b>			
ADE	$1.4 \pm 0.1$	$^2\text{A}_1 \rightarrow ^1\text{A}_1$	1.09
X	$1.68 \pm 0.1$	$^2\text{A}_1 \rightarrow ^1\text{A}_1$ ( $^2\text{A}_1$ VDE)	1.49
A	$1.80 \pm 0.1$	$^2\text{A}_1 \rightarrow ^3\text{A}_1$	1.63
B	$1.96 \pm 0.1$	$^2\text{A}_1 \rightarrow ^1\text{A}_1$	1.86
C	$2.07 \pm 0.1$	$^2\text{A}_1 \rightarrow ^3\text{A}_1$	2.02

The most elementary motif that can be observed in the solids is  $\text{MB}_2$ , and thus, we begin from the  $\text{MB}_2^{0/-}$  clusters (ions being included for experimental characterization with anion photoelectron spectroscopy). All clusters have  $\text{C}_{2v}$  symmetry, with the metal coordinating to the center of the B-B bond. However, they have markedly different B-B and M-B distances (see SI), indicating that metals affect the B-B bonding in different ways.  $\text{TiB}_2^-$  ( $^2\text{A}_1$ ) has a short R(B-B) of 1.56 Å;  $\text{ReB}_2^-$  has three competing configurations,  $^3\text{B}_2$  - R(B-B)=1.75 Å,  $^3\text{B}_1$  - R(B-B)=1.66 Å (2.51 kcal/mol above  $^3\text{B}_2$ ), and  $^3\text{A}_2$  - R(B-B)=1.76 Å (3.14 kcal/mol above  $^3\text{B}_2$ ).  $\text{OsB}_2^-$  ( $^4\text{A}_2$ ) has R(B-B) of 1.66 Å. Note that these calculations are large-active-space multireference with dynamic electron correlation (see SI). This tour-de-force theoretical approach appeared to be required to reproduce experimental spectra for these seemingly simple systems.<sup>16</sup> The close proximity and mixing of many electronic states can be linked to the promiscuity of metal-boron bonding. Table 1 and Figure 2 show the experimental and theoretical photoelectron spectra ( $\text{OsB}_2^-$  was not done experimentally due to the high toxicity of Os). The good agreement between theory and experiment signifies that theory can adequately describe these clusters, and provide an electronic structure insight.

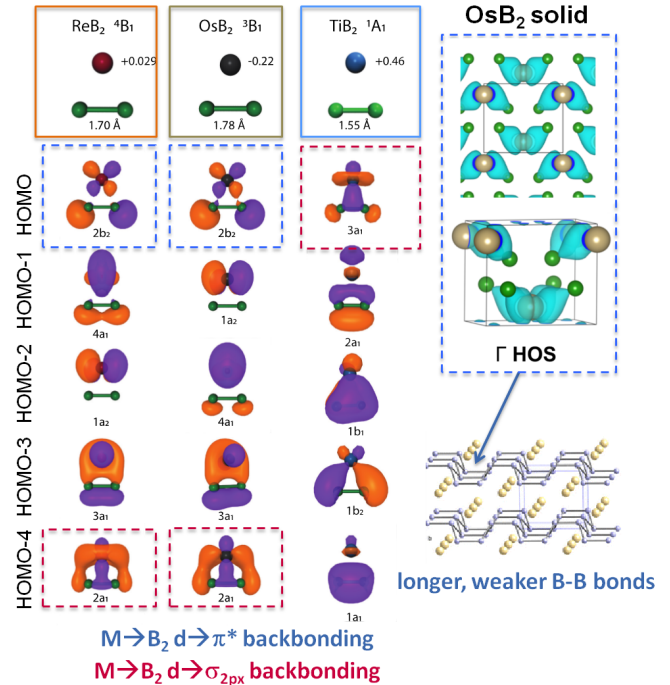


**Figure 3.** Left: The Kohn-Sham Orbitals of  $\text{ReB}_2$ ,  $\text{OsB}_2$ , and  $\text{TiB}_2$ , truncated set; NBO charges on atoms. The  $\text{d} \rightarrow \sigma_{2\text{px}}$   $\text{M} \rightarrow \text{B}_2$  backbonds are outlined in red, and  $\text{d} \rightarrow \pi^*$  - in blue. Right: The  $\text{d} \rightarrow \pi^*$  state occupied in solid  $\text{OsB}_2$ , corresponding to the donation from Os to the activated and elongated B-B bonds.

The chemical bonding in the three neutral clusters (Figure 3) reveals peculiarities of metal-boron interactions, and differences between the three clusters. When transition metals interact with  $B_2$ , the back-donation firstly happens to the LUMO of  $B_2$ , which is a bonding  $\sigma_{2px}$ -MO. The  $d\text{-AO}\rightarrow\text{LUMO}(B_2)$  back-donation thus strengthens the B-B bond. The resulting MO falls deep below the HOMO-LUMO gap in  $ReB_2$  and  $OsB_2$ , while in  $TiB_2$  it is the HOMO. In addition, Re and Os are capable of back-donation to the LUMO+1 ( $\pi^*$ ) of  $B_2$ , in the clusters' HOMOs.  $d\rightarrow\pi^*$  is bonding between the metal and  $B_2$ , and B-B  $\pi$ -antibonding. Due to this MO,  $R(B-B)$  in  $ReB_2$  and  $OsB_2$ , is elongated. Both back-bonds are lower in energy in  $OsB_2$  than in  $ReB_2$ , and, while this makes little difference for clusters, it will become profoundly important in the corresponding solids. Both types of back bonds are covalent in nature, as seen also from the partial charges on atoms (Figure 3). The ionic M- $B_2$  bonding component is the strongest in  $TiB_2$ . Thus, clusters give us a simple representation of the fundamental M- $B_2$  interactions possible in the three systems.

**Table 2.** Bader charges of metals in both **natural** and foreign crystal structures (optimized to the nearest stationary point).

	<b>Os</b>	<b>Re</b>	<b>Ti</b>
<b>Boat</b>	<b>+0.04</b>	+0.44	+2.02
<b>Chair</b>	+0.07	<b>+0.39</b>	+1.89
<b>Flat</b>	+0.60	+0.93	<b>+1.98</b>

In the bulk, the dangling valencies present in clusters are saturated, and so some cluster electronic states become unoccupied. The  $d\rightarrow\sigma_{2px}$  HOMO in  $TiB_2^{0/-}$  does not have an analog among the valent states in the bulk  $TiB_2$ . The material thus exhibits no covalent Ti-B interactions, and the only bonding present is ionic, as is also clear from the charge of +2 on Ti, corresponding to a typical  $d^2$  configuration (Table 2). Furthermore, the +2 charge persists when Ti is substituted into the boat or chair structures. The  $TiB_2$  structure type is also characteristic of diborides including Mg, V, Cr, Mn, Sc, Zr, Nb, and Mo.<sup>17</sup> The common electronic origin: the presence of a 2+ metal.  $M^{+2}$  means that the boron sublattice receives one electron per B. B<sup>-</sup> is isoelectronic to neutral C, and the flat hexagonal boron sheet is therefore isoelectronic and isostructural to graphene. In fact, it has many attributes of graphene, such as the Dirac points.<sup>18</sup>

Both  $ReB_2$  and  $OsB_2$  retain the  $d\rightarrow\sigma_{2px}$  states in the bulk, in line with their low energies in the cluster models. These states strengthen both M-B and B-B bonding. However, the  $d\rightarrow\pi^*$  state exists only in  $OsB_2$ , and specifically in the longer B-B bonds within the asymmetric

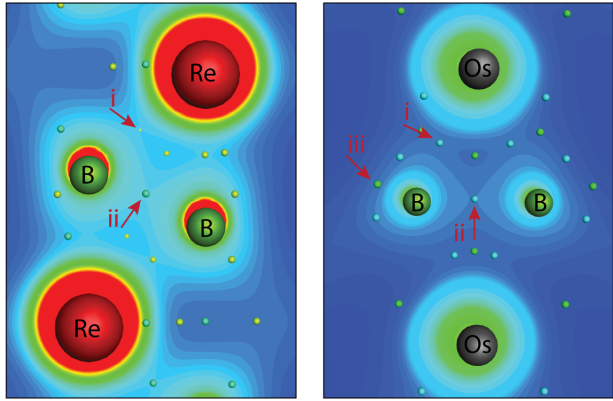


**Figure 4.** Electron density plots of  $ReB_2$  (left) and  $OsB_2$  (right). QTAIM CPs are indicated: bond CPs - blue, ring CPs - green, cage CPs - yellow. i - M-B CP, ii, iii - B-B CPs.

“boat” structure (Figure 3). Os has enough electrons to give only half of the B-B bonds a  $\pi^*$  character. Thus the “boat” structure of  $OsB_2$  is dictated by the antibonding M- $B_2$  interactions, which makes half of the B-B bonds longer and weaker, while in  $ReB_2$  all B-B bonds are strengthened by M-B interactions. The M-B bonds are stronger in  $OsB_2$ . Increased covalent character in Re and Os borides reflects in greatly reduced partial charges as compared to those in  $TiB_2$ , particularly in the Os systems (Table 2). Hence we see the chemical bonding origin of the structural differences of the three borides.

We further quantify the degree of covalency and relative bond strengths in the solids via the quantum theory of atoms in molecules (QTAIM) (Figure 4, Table 3), which analyzes the total rather than per-MO charge density.<sup>19,20</sup> QTAIM detects the presence of critical points (CPs) in the charge density. In the “boat” configuration, there are three bond CPs, labeled i (M-B CP), ii (B-B CP), and iii (the second B-B CP). The “chair” structure has two distinct bond CPs, i and ii. The amount of charge at bond CPs correlates with bond strength.<sup>21,22</sup> Both the “boat” and “chair” structures have stronger M-B bonds when containing Os rather than Re. Furthermore, while in general B-B bonds are stronger than M-B bonds the B-B bonds in  $OsB_2$  systems are of comparable strength to the Os-B bonds in contrast to the more differentiated  $ReB_2$  systems. Thus, the covalent character of Re/Os-B bonds is confirmed, and it is additionally seen that half of the B-B bonds in  $OsB_2$  are weakened by the interaction with Os, with the charge density flowing from B-B to Os-B bonds.

As a confirmation of the QTAIM analysis, we employed the COHP method to directly measure the bond strengths between the different atoms (See SI). The integrated COHP values indicate that in  $ReB_2$  Re-B bonds are much weaker than the corresponding B-B bonds

while in  $\text{OsB}_2$  Os-B bonds are stronger than the lengthened B-B bonds. This corroborates the QTAIM picture.

**Table 3.** : The charge densities (in  $e^-$ ) at the bond CPs for both Re and Os in the boat and chair structures.

	A	B	C
ReB <sub>2</sub> boat	0.608	0.740	0.697
OsB <sub>2</sub> boat	0.656	0.732	0.618
ReB <sub>2</sub> chair	0.590	0.713	X
OsB <sub>2</sub> chair	0.629	0.668	X

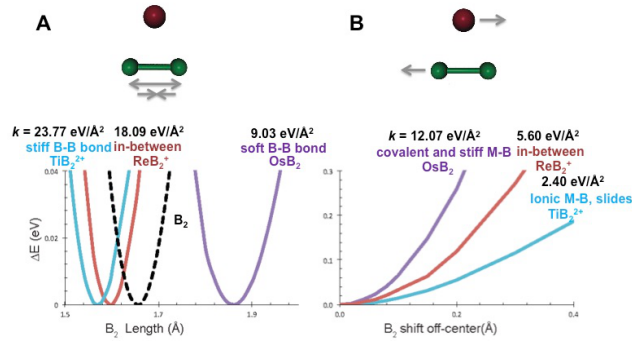


**Figure 5.** (A) Energies of the clusters as a function of (A) compression along the B-B bond, (B) shear distortion coordinate. Cyan -  $\text{TiB}_2^{2+}$ , Red -  $\text{ReB}_2^+$ , Purple -  $\text{OsB}_2$ , dashed black - isolated  $\text{B}_2$  for a reference.

There transpires a correlation between the relative strengths of the M-B and B-B bonding and materials' hardness. In order to pin it down, we depart from the static bonding picture constructed at equilibrium. Hardness is a response to external force, and the effect of pressure is comprised by the combination of two types of distortion: compression and shear. High incompressibility and shear modulus are both necessary, but not alone sufficient for hardness.<sup>5-10</sup> We examine the materials' response to these two types of stimuli independently, again relying on the cluster models for clarity.

Because the  $\pi^*$  back-bond is not present in the  $\text{ReB}_2$  and  $\text{TiB}_2$  solids, at this point, the clusters were charged +1 and +2, respectively, in order to unoccupy the  $d \rightarrow \pi^*$  states. To mimic the effects of compression and shear stress, the B-B compression and M-B<sub>2</sub> shift were applied, and the clusters' responses were monitored (Figure 5)<sup>23</sup> Response to compression should primarily report on the strength of the B-B bonding, whereas that to shear should report on the M-B bonding. The force constants corresponding to the  $\text{B}_2$  compression (Figure 5A) show bond stiffening in order of covalent to ionic char-

acter.  $\text{TiB}_2^{2+}$  has the stiffest B-B bond, because it is compact, and electrons confined to the smaller space resist the deformation, while the stable  $d^2 \text{Ti}^{2+}$  is not willing to relieve the stress by taking electrons back.  $\text{ReB}_2^+$ , with its  $d \rightarrow \sigma_{2px}$  back-bond, has a strengthened B-B bond, and some charge flow toward M-B bonds allowing for the flexibility in charge distribution. Thus, B-B bonds are slightly less stiff than in  $\text{TiB}_2^{2+}$ . Being the most covalent, Os is the other extreme: the B-B bond activation by the  $d \rightarrow \pi^*$  donation leads to charge redistribution toward the covalent Os-B bonds. The system is

**Table 4.** The calculated properties of Re and Os in both the boat and chair structures. G is the shear modulus. X indicates that the structure only has one  $\text{B}_2$  bond length.

	$\text{B}_2$ -1 (Å)	$\text{B}_2$ -2 (Å)	G (GPa)
OsB <sub>2</sub> -Boat	1.80	1.88	166
ReB <sub>2</sub> -Boat	1.84	1.81	244
OsB <sub>2</sub> -Chair	1.86	X	187
ReB <sub>2</sub> -Chair	1.82	X	276

further capable of relieving the stress by shifting electrons toward Os upon the B-B bond compression as if having a shock absorber both in the cluster and in every unit cell in the solid. This reduces material's stiffness upon compression.

The clusters' ordering of resistance to shearing is exactly the opposite from that to compressing (Figure 5B). The M-B<sub>2</sub> bonding is the most covalent in  $\text{OsB}_2$ , intermediate in  $\text{ReB}_2^+$ , and purely ionic in  $\text{TiB}_2^{2+}$ . Hence, Ti in  $\text{TiB}_2^{2+}$  easily slides along  $\text{B}_2$ ,  $\text{ReB}_2^+$  resists the slip more, and  $\text{OsB}_2$  is the most resilient because the slip disrupts the strong Os-B bonds.  $\text{OsB}_2$  has a force constant 5 times higher than that of  $\text{TiB}_2^{2+}$  for this mode of deformation. To bridge our understanding to the solids, we examine stiffness tensors (SI Tables 7-11). Starting with compression of the boron network ( $C_{11}$ ), we see  $\text{ReB}_2 \approx \text{TiB}_2 > \text{OsB}_2$ . This shows the same distinction we had in the clusters: Re and Ti stiffen B the same amount, and Os weakens it. Shearing the metal against the B sheet shows  $\text{ReB}_2$  ( $C_{55}$ ) >  $\text{TiB}_2$  ( $C_{44}$ ) >  $\text{OsB}_2$  ( $C_{66}$ ). This is not the same as the cluster model, but we must consider that there are other interactions in real distortions. The cluster model is Os bound to a long  $\text{B}_2$ , but in the solid there are also shorter, more slippery,  $\text{B}_2$  bonds. Still, it should be hardest to shear on that long  $\text{B}_2$  bond in  $\text{OsB}_2$  ( $C_{66}$ ), and that is the case. ( $C_{66} > C_{44} \gg C_{55}$ ). In  $\text{TiB}_2$  the shear across the B layer is the easiest ( $C_{44} < C_{66}$ ). Thus, we can explain slip-plane strength in solids.

Finally, we computed the geometries and shear moduli of Re and Os in both boat and chair configurations (Ta-

ble 4). The consequence of more covalent Os-B bonding is a lengthening of the B<sub>2</sub> bonds in the chair structure. This, in turn, lowers the shear modulus. Similarly, Re added to the boat structure causes B<sub>2</sub> bonds to move towards uniformly short, losing the antibonding  $\pi^*$  character, and increasing in the shear modulus. Os in the chair structure is significantly harder than its boat counterpart. This results from forcing the B-lattice to be uniform—no B<sub>2</sub> bond becomes overly covalent, but all are weakened. The moduli thus have full support from the cluster bonding models.

In conclusion, a metal that is too covalent with boron will lower the incompressibility, while a metal that is too ionic with boron will lower the shear strength. A ‘goldilocks metal’ would be intermediate, i.e. having only the bonding  $d \rightarrow \sigma_{2px}$  and no antibonding  $d \rightarrow \pi^*$  B-M bonds. Re within the given family of diborides has just the right electron count to fulfill this requirement; as a result ReB<sub>2</sub> is the only ultra hard boride. This constitutes a new bonding model for ultra hard borides, which is based on promiscuous metal-boron bonding, previously unrecognized as one of the crucial aspects of superhard structures. The model reveals the origin of the structural differences in the TiB<sub>2</sub>, ReB<sub>2</sub>, and OsB<sub>2</sub> borides, and explains their differences in hardness. Beyond the three borides, a chemical bonding based design principle for hard materials is a step towards designing novel materials that rival diamond’s hardness.

## ASSOCIATED CONTENT

### Supporting Information

Theoretical Methods, Experimental Methods, Experimental and Simulated Mass Spectra of ReB<sub>2</sub><sup>-</sup> and TiB<sub>2</sub><sup>-</sup>, Alternate Minima and Excited States of Clusters, Elastic Moduli of Structures, Elastic Tenors of Structures, COHP analysis  
The Supporting Information is available free of charge on the ACS Publications website.

## AUTHOR INFORMATION

### Corresponding Author

K. H. Bowen. email: [kbowen@jhu.edu](mailto:kbowen@jhu.edu)

A. N. Alexandrova. email: [ana@chem.ucla.edu](mailto:ana@chem.ucla.edu)

### Author Contributions

PJR and ANA conceived the project and performed the theoretical investigation; GL, SMC, and KHB designed and carried out the experiments; CJMM, JRC, and TMM prepared the rhenium boride rod. PJR and ANA drafted the manuscript. All authors assisted in editing the manuscript.

## ACKNOWLEDGMENT

We thank Garth Billings of Diversified Advanced Technologies, LLC (9310 Prototype Drive, Reno, NV 89521, 775-857-4300, [garth.billings@sbcglobal.net](mailto:garth.billings@sbcglobal.net)) for providing the ReB<sub>2</sub> sample. We thank Professors Richard Kaner Professor Sarah Tolbert and Dr. Michael Yeung for a helpful dis-

cussion. This work was supported by the Air Force Office of Scientific Research (AFOSR) under Grant FA9550-15-1-0259 (K.H.B.), NSF Career Award CHE1351968 (A.N.A.), the Johns Hopkins University Catalyst Fund (T.M.M.), the NSF’s PARADIM (Platform for the Accelerated Realization, Analysis, and Discovery of Interface Materials) program, a Materials Innovation Platform (T.M.M.) and the donation of Ms. Evers-Manly for the Undergraduate Research Scholars Program in UCLA (P.J.R.). UCLA IDRE cluster Hoffman2 was used for all calculations.

## REFERENCES

- (1) H.Y. Chung, M.B. Weinberger, J.B. Levine, A. Kavner, J.M. Yang, S.H. Tolbert, R.B. Kaner. Synthesis of Ultra-Incompressible Superhard Rhenium Diboride at Ambient Pressure. *Science* **2007**, *316*, 436-439
- (2) R.W. Cumberland, M.B. Weinberger, J.J. Gilman, S.M. Clark, S.H. Tolbert, R.B. Kaner. Osmium Diboride, an Ultra-Incompressible, Hard Material. *J. Am. Chem. Soc.* **2005**, *127*, 7264-7265
- (3) R.B. Kaner, J.J. Gilman, S.H. Tolbert. Designing Superhard Materials. *Science* **2005**, *308*, 1268-1269
- (4) A.T. Lech, C.L. Turner, R. Mohammadi, S.H. Tolbert, R.B. Kaner. Structure Of Superhard Tungsten Tetraboride: A Missing Link Between MB<sub>2</sub> And MB<sub>12</sub> Higher Borides. *Proc. Natl. Acad. Sci. U.S.A* **2015**, *112*, 3223-3228.
- (5) J.B. Levine, S.H. Tolbert, R.B. Kaner. Advancements in the Search for Superhard Ultra-Incompressible Metal Borides. *Adv. Funct. Mater.* **2009**, *19*, 3519-3533.
- (6) J. J. Gilman, R. W. Cumberland, R. B. Kaner. Design of Hard Crystals. *Int. J. Refract. Met. Hard Mater.* **2006**, *24*, 1-5
- (7) V. V. Brazhkin, A. G. Lyapin, R. J. Hemley. Harder Than Diamond: Dreams and Reality. *Philos. Mag. A* **2002**, *82*, 231-253
- (8) J. Haines, J. M. Léger, G. Bocquillon. Synthesis and Design of Superhard Materials. *Annu. Rev. Mater. Res.* **2001**, *31*, 1-23.
- (9) J. M. Leger, P. Djemia, F. Ganot, J. Haines, A. S. Pereira, J. A. H. da Jornada. Hardness and Elasticity in Cubic Ruthenium Dioxide. *Appl. Phys. Lett.* **2001**, *79*, 2169-2171
- (10) W. A. Harrison, *Electronic Structure and the Properties of Solids*, Freeman, San Francisco **1980**.
- (11) M.T. Yeung, R. Mohammadi, R.B. Kaner. Ultrahardness, Superhard Materials. *Annu. Rev. Mater. Res.* **2016**, *46*, 465-485
- (12) Q. Gu, G. Krauss, W. Steurer. Transition Metal Borides: Superhard Versus Ultra-incompressible. *Adv. Mater.* **2008**, *20*, 3620-3626
- (13) R. G. Munro. Material Properties of Titanium Diboride. *J. Res. Natl. Inst. Stand. Technol.* **2000**, *105*, 709-720
- (14) R. Hoffmann, *Solids and surfaces: a chemist's view of bonding in extended structures*, VCH Publishers, **1988**
- (15) R. Hoffmann, C. Zheng. Making and Breaking Bonds in the Solid State: The ThCr<sub>2</sub>Si<sub>2</sub>, Structure. *J. Phys. Chem.*, **1985**, *89*, 4175-4181
- (16) P. J. Robinson, X. Zhang, T. McQueen, K. H. Bowen, A. N. Alexandrova. SmB<sub>6</sub><sup>-</sup> Cluster Anion: Covalency Involving f Orbitals. *J. Phys. Chem. A* **2017**, *121*, 1849-1854.
- (17) G. Akopov, M. T. Yeung, R. B. Kaner. Rediscovering the Crystal Chemistry of Borides. *Adv. Mater.* **2017**, *29*, 1604506.
- (18) X. Feng, C. Yue, Z. Song, Q. Wu, B. Wen. Topological Dirac Nodal-net Fermions in AlB<sub>2</sub>-type TiB<sub>2</sub> and ZrB<sub>2</sub>. arXiv:1705.00511, **2017**
- (19) A. Morgenstern, T. Wilson, J. Miorelli, T. Jones, M. E. Eberhart. In Search of an Intrinsic Chemical Bond. *Comp. Theor. Chem.* **2015**, *1053*, 31-37
- (20) R. F. Bader, *Atoms in Molecules*. John Wiley & Sons, **1990**

(21) C.F. Matta, R.J. Boyd, *The Quantum Theory of Atoms in Molecules: From Solid State to DNA and Drug Design*, John Wiley & Sons, **2007**

(22) S.J. Grabowski. Ab Initio Calculations on Conventional and Unconventional Hydrogen Bonds—Study of the Hydrogen Bond Strength. *J. Phys. Chem. A* **2001**, 47, 10739-10746

(23) P. J. Robinson, A. N. Alexandrova. Assessing the Bonding Properties of Individual Molecular Orbitals. *J. Phys. Chem. A* **2015**, 119, 12862-12867.

TOC Graphics:

